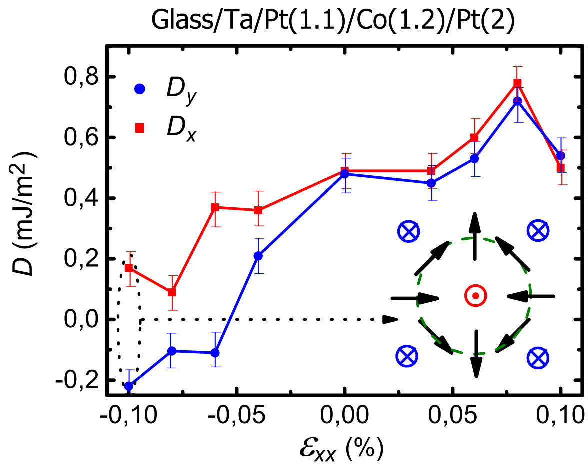

FIG. 5. The DMI constant measured along the x- and y-directions ($D_{x,y}$) as a function of applied strain (ε_{xx}) for the sample with $d_{\rm Pt}$ = 1.1 nm. See the linear least-square fits in the Supplementary materials. The inset shows the skyrmion with an antivortex domain wall. It may appear due to the anisotropic DMI with different sign along different directions [30].

TABLE I. DMI interaction constants for different samples. The first three lines show the data for the sample in Fig. 3 and 5. The last two lines show the data for two additional samples. The constants D_{0x}, D_{0y} are measured in mJ/m^2, D_1, $D_{\rm an}$ are measured in mJ/(m^2(%)). The samples thickness is defined with the precision of 20%.

$d_{\rm Pt}$, nm	Anis.	D_{0x}	D_{0y}	D_1	$D_{\rm an}$	$D_1 + D_{\rm an}$
0.4	in-plane	0.27±0.03	-	-	-	0.7±0.6
1.1	mixed	0.43 ±0.08	0.3 ±0.1	3.4 ±1.1	-0.9 ±0.6	2.5 ±1.1
1.9	mixed	0.4 ±0.05	0.2 ±0.1	3.2 ±0.7	-1 ±0.8	2.5 ± 1.4
2	mixed	0.42 ±0.02	0.4 ±0.03	2.1 ±1	-0.5 ±0.3	1.6 ±0.8
2.2	perp.	0.42±0.03	-	-	-	1.1±0.8

the expression

$$W_{\rm DMI} = D_x\left(m_x\frac{\partial m_z}{\partial x} - m_z\frac{\partial m_x}{\partial x}\right) + D_y\left(m_y\frac{\partial m_z}{\partial y} - m_z\frac{\partial m_y}{\partial y}\right). \quad (3)$$

In the linear approximation the constants $D_{x,y}$ can be expressed via strain as follows

$$D_{x,y} = D_{0x,y} + D_1(\varepsilon_{xx} + \varepsilon_{yy}) \pm D_{\rm an}(\varepsilon_{xx} - \varepsilon_{yy}), \quad (4)$$

where the tensor ε is the strain in the film, the sign "+" ("-") is for D_x (D_y). The first term describes the anisotropic DMI in the unstrained film, the second term shows the influence of the isotropic strain and the third contribution represents the effect of the anisotropic deformation.

Using a linear least-squares fit (see Supplementary materials) of our data we get the constants D_{0x}, D_1, and $D_{\rm an}$ for our samples. The obtained results are summarized in the Table I. First three lines are for samples shown in Fig. 3. Two bottom lines are for two additional samples mentioned above. The second column indicate the anisotropy type in each sample. Two additional samples studied here have the "mixed" type of magnetic hysteresis loop similar to the sample with $d_{\rm Pt} = 1.1$ nm. While the uncertainty of the data is quite hight, all the samples have non zero sensitivity to the strain (see $D_1 + D_{\rm an}$). The samples with the mixed anisotropy type ($d_{\rm Pt} = 1.1$ nm and $d_{\rm Pt} = 1.9$ nm) have the highest average sensitivity. The mixed type of the anisotropy and high average $D_1 + D_{\rm an}$ appear in the samples with intermediate Pt thickness. The samples with thin small ($d_{\rm Pt} = 0.4$ nm) and high ($d_{\rm Pt} = 2.2$ nm) Pt thickness have lower strain sensitivity. The films with the mixed anisotropy type demonstrate strong DMI anisotropy also (see $D_{\rm an}$).

The strain induced in our films due to the bending of the samples is of order of 0.1%. Such a value can be easily achieved in ferroelectric crystals under application of voltage. For example, in $Pb(Mg_{1/3}Nb_{2/3})O_3PbTiO_3$ (PMN-PT) crystal the voltage induced strain reaches 0.3% [31] which is even higher than what we use in our experiments. So, one can control DMI with voltage in ferroelectric/(Co/Pt) systems. Assuming linear dependence of the DMI coefficient on ε one can expect modulation of the DMI constant from -0.8 to 1.8 mJ/m^2 in the electric field range of about ±600 V/mm in PMN-PT/Ta/Pt/Co/Pt system. Note that for certain cut of PMN-PT crystal the induced strain is highly anisotropic. So, the voltage controlled DMI anisotropy can be realized.

To understand the correlation between the strain-induced DMI variations in Fig. 3 and the magnetization curves transformations in Fig. 2c, we carried out micromagnetic simulations using the OOMMF code [32]. The results are shown in Fig. 2d. In the simulations we assumed the isotropic DMI varying with the strain similarly to what we observed in our BLS experiments (D_0 = 0, 0.5, and 1 mJ/m^2). The saturation magnetization $M_{\rm s} = 1.1 \cdot 10^6$ A/m and the exchange stiffness $A = 2 \cdot 10^{11}$ J/m [28] were uniform across the film. The magnitude of the perpendicular uniaxial anisotropy varies across the sample between $K_{\rm min} = 6.3 \cdot 10^5$ J/m^3 and $K_{\rm max} = 8.3 \cdot 10^5$ J/m^3. These values are near the critical anisotropy $K = \mu_0 M_{\rm s}^2/2 = 7.6 \cdot 10^5$ J/m^3 corresponding to the easy plain - easy axis transition. The parameters used are in agreement with what we obtained from fitting of BLS data. The BLS data confirms also that the anisotropy varies weakly with strain (see Supplementary materials).

Increasing the DMI reduces the domain wall energy and increases the magnetic field at which domains disappear (the hysteresis loop width). This is in agreement with our experimental observations (Fig. 2). So, we conclude that the magnetization loops variations observed